УДК 004.932 https://doi.org/10.15407/vidbir2024.52.095

LOCAL IMAGE CONTRAST ENHANCEMENT BASED ON POWER MODEL OF VISUAL IMAGE PERCEPTION

R. A. Vorobel [1], O. R. Berehulyak [1], I. B. Ivasenko [1,2], T. S. Mandziy [1]

[1] H. V. Karpenko Physico-Mechanical Institute of the NAS of Ukraine, Lviv;

[2] Lviv Polytechnic National University, Lviv

E-mail: roman.vorobel@gmail.com, olena.berehulyak@gmail.com, ivasenko.iryna@gmail.com, teodor.mandziy@gmail.com

The analysis of models of light perception by humans, which serve as the basis for building methods for improving the quality of images by enhancing their local contrasts, was carried out. It is shown that the expression for determining local contrast is the basis for building an algorithm for image quality improvement. Three types of local contrast are highlighted, in particular absolute, relative and weighted, and the technology of building a method of image quality enhancement using them is illustrated. A new method of image quality improvement, which is based on the power dependence of the response of the human visual system to light excitation, is described. The experimental study of its effectiveness, illustrated and confirmed by image quality assessment, is carried out.

Keywords: *image processing, local contrast, power enhancement, visual perception of light*.

ПІДСИЛЕННЯ ЛОКАЛЬНИХ КОНТРАСТІВ ЗОБРАЖЕННЯ НА ОСНОВІ СТЕПЕНЕВОЇ МОДЕЛІ ЙОГО ЗОРОВОГО СПРИЙНЯТТЯ

Р. А. Воробель [1], О. Р. Берегуляк [1], І. Б. Івасенко [1,2], Т. С. Мандзій [1]

[1] Фізико-механічний інститут ім. Г. В. Карпенка НАН України, Львів;

[2] Національний університет “Львівська політехніка”

Оброблення зображень у просторовій області для підвищення їх візуальної якості характеризується відносною простотою та швидкодією. Водночас підсилення локальних контрастів у просторовій області є основним компонентом поліпшення якості зображення. Проаналізовано моделі сприйняття світла людиною, які є основою для побудови методів поліпшення якості зображень внаслідок підсилення їх локальних контрастів. Показано, що вираз для визначення локального контрасту є базою для побудови алгоритму покращення якості зображення. Виділено три типи локального контрасту (абсолютний, відносний і зважений) та проілюстровано технологію побудови методу підвищення якості зображення з їх використанням. Однак згадані методи не забезпечують рівномірності підсилення контрасту як для висококонтрастних ділянок зображення, так і для низькоконтрастних. Запропоновано новий метод поліпшення якості зображення, який базується на степеневій залежності реакції зорової системи людини на світлове збудження. Виконано експериментальне дослідження його ефективності порівняно з відомими методами. Результати досліджень проілюстровано на тестових зображеннях. Переваги запропонованого методу підтверджено оцінкою якості зображення, яка базується на чотирьох характеристиках монохромного напівтонового зображення – відхиленні узагальненого абсолютного контрасту від його середнього значення, оцінках рівня адаптації зорової системи людини за яскравістю під час сприйняття зображення, повноти використання градацій сірого та різкості. Цей метод показує кращі візуальні результати в широкому динамічному діапазоні інтенсивностей зображення порівняно з відомими методами на основі абсолютного, відносного та зваженого локального контрасту та забезпечує рівномірність підсилення як для висококонтрастних ділянок зображення, так і для низькоконтрастних.

Ключові слова: *оброблення зображень, локальний контраст, степеневе підсилення, візуальне сприйняття світла*.

Introduction. A wide application of robotic mobile systems for industry, medicine, geology and everyday life requires the development of effective means of improving

the quality of images almost in real time of their registration [1–2]. At the same time, the enhancement of their local contrasts in the spatial domain is the basic component of image quality improvement. It is the image processing in the spatial domain that is characterized by relative simplicity and speed.

In [3] the author proposed a new local image enhancement technique which is based on a logarithmic mapping function. The shape of mapping is adaptable to the local luminance characteristics around each pixel. The mapping function combines logarithmic, identity and inverted logarithmic mappings. Such an approach permits simultaneous enhancement of the image luminance in bright and dark regions in the image. This is achieved by using logarithmic mapping for dark image regions and inverted logarithmic mapping for bright image regions.

In [4] authors conducted comprehensive survey of image contrast enhancement techniques in spatial domain. To compare performance of the methods qualitatively and quantitatively they used different performance measures designed for image quality assessment. Authors highlighted absolute mean brightness error (AMBE) and entropy as most commonly used image enhancement performance measure. Performance of the image enhancement method is also compared by their ability to preserve the main features of the image which reflect its quality. They consider such features as entropy and brightness preservation, loss of structural information and so on. Among various image datasets, which are used by different researchers for testing of their algorithms, authors mention USC-SIPI database as the most widely used one. It is shown that recursive median and mean partitioned one-to- one gray level mapping transformations for image enhancement (RMMGHT) is the method that preserves entropy and provides minimal AMBE. As the overall conclusion the authors state that different image enhancement approaches have different advantages and should be selected based on user requirements.

However, known methods of enhancing local contrasts, which are based on the use of absolute, relative or weighted contrasts [5-6], do not ensure the uniformity of this enhancement in a wide dynamic range of image intensities. Therefore, it is relevant to develop a method of enhancing local contrasts which uses a power model of image perception as a means of visual stimulation in a wide range of its intensities.

Basic models of human light perception. The reaction of the visual system to changes in intensities in their wide range is the basic component of the quantitative determination of changes in observed intensities. The main dependence here [7] is logarithmic-linear. It satisfactorily predicts the psychophysical reaction of a person to light excitation and is described by the expression

$$I_{out}(x,y) = K_1 \ln\left[K_2 + K_3 I_{in}(x,y)\right], \tag{1}$$

where K_1, K_2, K_3 are constants and $I_{in}(x,y)$ and $I_{out}(x,y)$ are input and output signal, respectively. Other models are also known [8]. They describe the reaction with the expression

$$I_{out}(x,y) = \frac{K_1 I_{in}(x,y)}{K_2 + I_{in}(x,y)}, \tag{2}$$

where K_1, K_2 are constants. In [5] Mannos and Sakrison studied various nonlinearities, used in analytical measures of validity of image reproduction. They defined the power nonlinearity as

$$I_{out}(x,y) = \left[I_{in}(x,y)\right]^R, \tag{3}$$

where R is a constant. It provides good agreement between the calculated validity and the subjective assessment of image quality. The paper [7] describes the basic points of human perception of light. In particular, a source of white ligh L_1 is considered which has a brightness Y and is located in the immediate vicinity to the second source of white light L_2 with the same spectrum and brightness $Y + \Delta Y$. Measurements of contrast sensitivity showed that the Weber ratio $\Delta Y/Y$ i.e. the ratio of a barely noticeable brightness difference to the absolute brightness value Y in a sufficiently wide range of values Y, is almost constant and equal to 1...2% [7]. On this basis, it can be asserted that the increase in lightness of the second source in relation to the first should be determined by a logarithmic expression

$$\Delta\{L_1, L_2\} = \log_b(Y + \Delta Y) - \log_b(Y), \tag{4}$$

and not by the difference in brightness ΔY. Since the differential of the logarithm of brightness is equal

$$d\left[\log_b(Y)\right] = \lim_{\Delta Y \to 0}\left[\log_b(Y + \Delta Y) - \log\right] = \log_b(e)\frac{dY}{Y}, \tag{5}$$

then the increase in the logarithm of brightness is equal to the Weber ratio (e – Euler's constant). Mannos and Sakrison [8] studied the possibilities of changing the validity of reproduction of grayscale images using expression (3). In this case, the following value becomes the measure of lightness increase

$$\Delta\{L_1, L_2\} = (Y + \Delta Y)^{\nu} - (Y)^{\nu}, \tag{6}$$

where ν is a constant. Cornsweet in his study [9] assumed that the response of photo-receptors of the retina was described by a nonlinear rule (3). Then the corresponding measure of lightness increase is calculated as

$$\Delta\{L_1, L_2\} = \frac{K_1(Y + \Delta Y)}{K_2 + (Y + \Delta Y)} - \frac{K_1 Y}{K_2 + Y}, \tag{7}$$

where K_1, K_2 are constants.

Measures (4), (6) and (7) belong to local measures of lightness change. Global measures are also often used to compare the brightness of strongly different light sources. Such measures were obtained on the basis of empirical models built on experimental material. In particular, Priest, Gibson and McNicholas [10] proposed a simple relationship

$$\Lambda = Y^{\frac{1}{2}}, \tag{8}$$

where the brightness Y changes from 0 to 100, and luminance varies from 0 to 10. Ladd and Pinney [11] used a cube root scale

$$\Lambda = 2,468 \cdot Y^{\frac{1}{3}} - 1,636, \tag{9}$$

where the brightness Y also changes from 0 to 100. In addition to these dependences, Foss [8] introduced a logarithmic scale

$$\Lambda = \lg Y + 0,25. \tag{10}$$

Judd [9] introduced a luminance scale which took background illumination Y_B into account. In this case, luminance was determined by the expression

$$\Lambda = \frac{0{,}1 \cdot Y\left(Y_B + 100\right)}{Y_B + Y}. \tag{11}$$

At the same time, it should be noted that Judd's empirical scale is similar in form to expression (7), which describes the non-linear model of photoreceptor response.

Mokrzycki and Tatol [12] presented the most popular linear and nonlinear color models and compared to the sample values. The problem of measuring the color difference was investigated. It was concluded that not all color spaces are suitable for uniform color measurement. Authors come to a conclusion that CIELAB is the most suited for precise measurements. Newer varieties of Euclidian distance for precise measurements were introduced.

Liberini and Rizzi [13] compared Munsell and Ostwald colour spaces for practical applications. They propose to use Munsell colour-ordering system as a tool for measuring hair colour appearance in different conditions stable in the case of light reflection.

Taking into account the above-described models of light perception by humans, let's consider the power model. We assume it is a two-component model, which uses low-frequency and high-frequency components as the basic ones. Therefore, at the beginning, we will show how the analytical expression of local contrast serves to build a method for improving image quality.

Methods of image enhancement by strengthening their local contrasts. To illustrate the method of improving the image quality by enhancing its local contrasts, we will choose three types of them – absolute, relative and weighted.

Method based on absolute local contrast. Absolute local contrast C_1 is described by the difference between the intensity of an image pixel L and the average intensity $\bar{L}$ of its neighbor pixels W

$$\bar{L} = \underset{L \in W}{mean}(L) \tag{12}$$

as

$$C_1 = \frac{L - \bar{L}}{LMAX}, \tag{13}$$

where $C_1 \in [0,1]$ $LMAX$ is the maximum possible value of the gray level of a pixel. Then from (13) we obtain

$$L = \bar{L} + sign\left(L - \bar{L}\right) \cdot LMAX \cdot C_1. \tag{14}$$

Then, enhancing the local contrast C_1 so that its new value C_1^* meets the requirement

$$\left|C_1^*\right| > \left|C_1\right|, \tag{15}$$

we form a new value L^* of intensity L

$$L^* = \bar{L} + sign\left(L - \bar{L}\right) \cdot LMAX \cdot C_1^*. \tag{16}$$

The obtained expression (16) proves that the absolute local contrast (13) is the basis of the synthesis of the unsharp masking method, which consists in forming a new intensity of the image pixel L^* as the sum of the low-frequency component $\bar{L}$ (12) and the amplified high-frequency component C_1^*.

Method based on relative local contrast. Relative local contrast C_2 is described by the expression

$$C_2 = \frac{L - \bar{L}}{L}, \tag{17}$$

for $L \geq \bar{L}$ wherefrom

$$L = \frac{\bar{L}}{1 - C_2}. \tag{18}$$

Enhancing the local contrast C_2 so that its new value C_2^* matches the requirement

$$\left|C_2^*\right| > \left|C_2\right|, \tag{19}$$

we form a new value L^* of intensity L which is described by the expression

$$L^* = \frac{\bar{L}}{1 - C_2^*}, \tag{20}$$

and for the case $\bar{L} > L$ by the expression

$$L^* = \bar{L}\left(1 - C_2^*\right). \tag{21}$$

Combining expressions (18) and (21), we have

$$L^* = \bar{L} \cdot \left(1 - C_2^*\right)^{sign\left(\bar{L} - L\right)}. \tag{22}$$

The obtained expression (22) represents the method of the relative local contrast enhancement [5,6].

Method based on weighted local contrast. Weighted local contrast C_3 is described by the expression

$$C_3 = \frac{L - \bar{L}}{L + \bar{L}}, \tag{23}$$

for $L \geq \bar{L}$ wherefrom

$$L = \bar{L}\frac{1 + C_3}{1 - C_3}. \tag{24}$$

Applying the local contrast C_3 enhancement described above, we form its new value

$$\left|C_3^*\right| > \left|C_3\right| \tag{25}$$

and, accordingly, the new value L^* of intensity L (24), which is written as

$$L^* = \bar{L}\frac{1 + C_3^*}{1 - C_3^*}, \tag{26}$$

and for the case $\bar{L} > L$

$$L^* = \bar{L}\frac{1 - C_3^*}{1 + C_3^*}. \tag{27}$$

Combining expressions (26) and (27) we get

$$L^* = \bar{L}\left(\frac{1 + C_3^*}{1 - C_3^*}\right)^{sign\left(\bar{L} - L\right)}. \tag{28}$$

Expression (28) represents the weighted local contrast enhancement method.

However, the local contrast enhancement methods (16), (22), (28) described above do not ensure the uniform enhancement of both high-contrast areas of the image and low-contrast areas. To eliminate this shortcoming, we built another method, which is based on the power-law formation of the reaction of the human visual system [14, 15]. We will describe it below.

A new method of power enhancement of local image contrasts. In the method developed by us, the local contrast is described by the expression

$$C_4 = \frac{\ln L - \ln \bar{L}}{\ln L} \tag{29}$$

for the case $L > \bar{L}$. This method also uses the local contrast enhancement, which is described by the expression

$$\left|C_4^*\right| > \left|C_4\right|. \tag{30}$$

From the expression (29), we determine the quantity L and obtain that it is described by the expression

$$L = \exp\left[\frac{\ln \bar{L}}{\left(1 - C_4\right)}\right], \tag{31}$$

and for the case of the enhanced local contrast, from the value C_4 to C_4^*, we get a corresponding new value L as L^*:

$$L^* = \exp\left[\frac{\ln \bar{L}}{\left(1 - C_4^*\right)}\right] = \bar{L}^{\frac{1}{\left(1-C_4^*\right)}}. \tag{32}$$

For the case $\bar{L} > L$ the expression for the local contrast is as follows

$$C_4 = \frac{\ln \bar{L} - \ln L}{\ln \bar{L}}, \tag{33}$$

wherefrom

$$L = \exp\left[\left(1 - C_4\right) \cdot \ln \bar{L}\right]. \tag{34}$$

Taking into account the enhancement of the local contrast (33) from C_4 to C_4^* we have

$$L^* = \exp\left[\left(1 - C_4^*\right) \cdot \ln \bar{L}\right] \tag{35}$$

or

$$L^* = \bar{L}^{\left(1-C_4^*\right)}. \tag{36}$$

We can combine the obtained expressions (32) and (36) into one

$$L^* = \bar{L}^{\left(1-C_4^*\right)^{sign\left(\bar{L}-L\right)}}. \tag{37}$$

The obtained expression (37) demonstrates exactly the power dependence of the influence of local contrast on the general procedure for image quality enhancement.

Image quality estimation. To evaluate the results of application of some image enhancement method not only qualitatively but also quantitatively the image quality

estimation metrics should be used [6]. Those metrics are divided into two classes which evaluate image with [16–18] or without [19, 20] the reference.

Choi and Bovik [21] presented estimation called Flicker Sensitive–Motion-based Video Integrity Evaluation (FS-MOVIE). This estimation computes filter responses on both reference and corrupted videos on Gabor filters and deploys them through energy model of motion perception and normalization. This estimation responses to the spectral separations. The quality assessment is a combination of internal flicker visibility index and motion-tuned measurements. It was tested on 4 databases. Experimental results confirmed that the estimation correlates with human judgments of video quality.

Ding et al [22] presented a full-reference image quality assessment method of deep image structure and texture similarity. It is based on the pre-trained VGG (Visual Geometry Group) network for object recognition. They computed the global means of convolution responses at each stage and established a universal parametric texture model. The parameters of the proposed measure are optimized using human ratings of image quality, and at the same time they minimize the distances between subimages. The proposed model provides good predictions of human quality ratings, is robust to such geometric transformations as translation and dilation.

In work [23], authors built models to learn content and quality-aware image representations for no-reference image quality assessment on real images. They used a Mixture of Experts approach to train of two encoders, that learn high-level content and low-level image quality features accordingly. This approach allows making image quality predictions compatible with CNN and traditional models. Authors also propose a novel scheme for low-level image quality representation learning. Experimental results demonstrated state-of-the-art performance. The proposed framework is flexible to the changes and can be extended to other CNN architectures.

We will evaluate the image without a reference [6, 24]. The quantitative evaluation of image quality is the product of four parameters of monochrome grayscale image

$$Q = 100 \cdot KC \cdot LQ \cdot KQ \cdot RQ, \tag{38}$$

where KC is the deviation of the generalized absolute contrast from its mean value, LQ is the assessment of the level of adaptation of the human visual system by the brightness during the perception of the image, KQ is the estimation of the completeness of the use of gray levels, RQ is the estimation of the sharpness.

Deviation of the generalized absolute contrast from its mean value is calculated as

$$KC = 1 - \left| 0,5 - C_{gen}^{abs} \right|, \tag{39}$$

where C_{gen}^{abs} is the generalized absolute contrast of gray scale image with eight-bit per pixel

$$C_{gen}^{abs} = \frac{1}{510} \sum_{L=0}^{255} \left| 2\left| L - \bar{L} \right| + 255 - \left| 2\left| L - \bar{L} \right| - 255 \right| \right| H\left(L\right) \tag{40}$$

and $H\left(L\right)$ is the histogram.

The level of adaptation of the human visual system by the brightness during the perception of the image is estimated as follows

$$LQ = 1 - \frac{2\left| \bar{L} - 0,5G \right|}{G}, \tag{41}$$

where $G = K - 1 = 2^n - 1$ and $n = 8$ is the number of bits per pixel.

Completeness of the use of gray levels is calculated by a formula

$$KQ = \frac{S}{G}, \tag{42}$$

where S is the number of gray levels, the number of pixels equal to which in the image is greater than the threshold $\beta \cdot N \cdot M$ ($\beta = 0.001$, N and M are the number of rows and columns).

Sharpness is estimated as follows

$$RQ = 1 - \exp\left(\frac{RR}{20}\right), \tag{43}$$

where

$$RR = \int_a^b \left(f(a) - f(b) \right)^{-1} \left(\frac{df(x)}{dx} \right)^2 dx, \tag{44}$$

$f(x)$ is a signal; a and b are the points located on the opposite edges of the level change.

Such estimator (38) was chosen for the evaluation of grayscale images quality since it essentially contains four different assessments which are versatile and comprehensive in determining the quality level of a given image.

Experimental results. The experimental results are given to demonstrate the effectiveness of the proposed method of power enhancement of local image contrasts. In particular, in Figures 1–4 the test images of Cameraman (Fig. 1*a*), Pout (Fig. 2*a*), Tire (Fig. 3*a*) and Moon (Fig. 4*a*) are presented as well as results of their enhancement by the method based on absolute local contrast (16) – Fig. 1–4*b*, method based on relative local contrast (22) – Fig. 1–4*c*, method based on weighted local contrast (27) – Fig. 1–4*d* and the proposed new method of power enhancement of local image contrasts (37) – Fig. 1–4*e*. The contrast is enhanced by an exponential function with a power equal to 0.8.

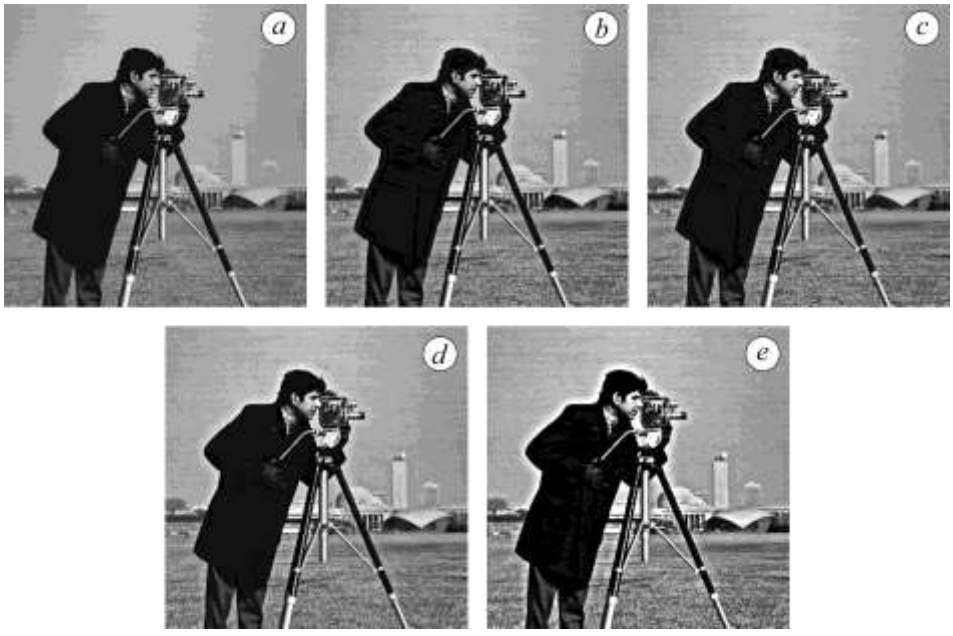

Fig. 1. Input Cameraman test image (*a*) and results of its enhancement by (16) (*b*), (22) (*c*), (27) (*d*) and proposed method (37) (*e*).

Fig. 2. Input Pout test image (*a*) and results of its enhancement by (16) (*b*), (22) (*c*), (27) (*d*) and proposed method (37) (*e*).

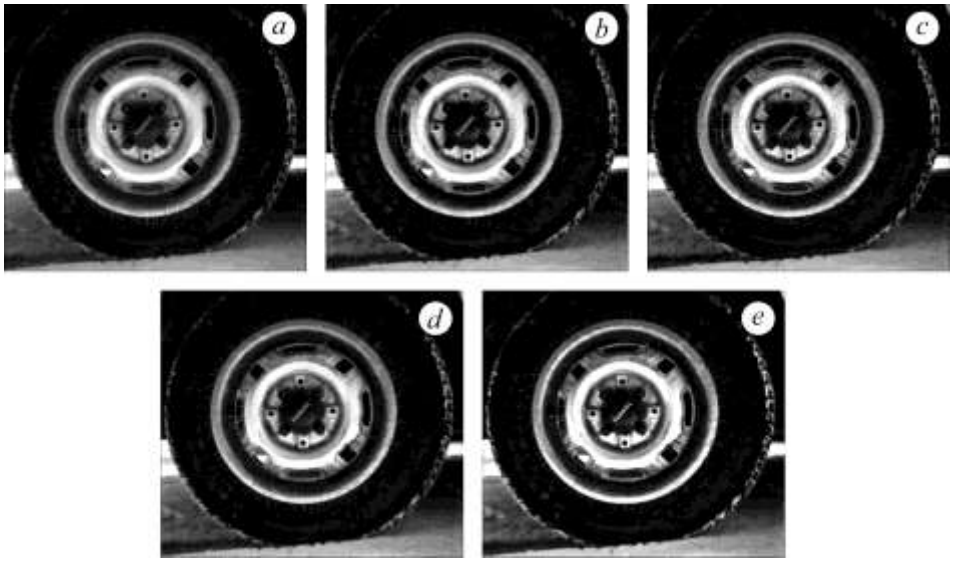

Fig. 3. Input Tire test image (*a*) and results of its enhancement by (16) (*b*), (22) (*c*), (27) (*d*) and proposed method (37) (*e*).

The proposed method shows better visual results in a wide dynamic range of image intensities compared to known methods based on absolute, relative local and weighted local contrast and ensures the uniformity of enhancement for both high-contrast areas of the image and low-contrast areas.

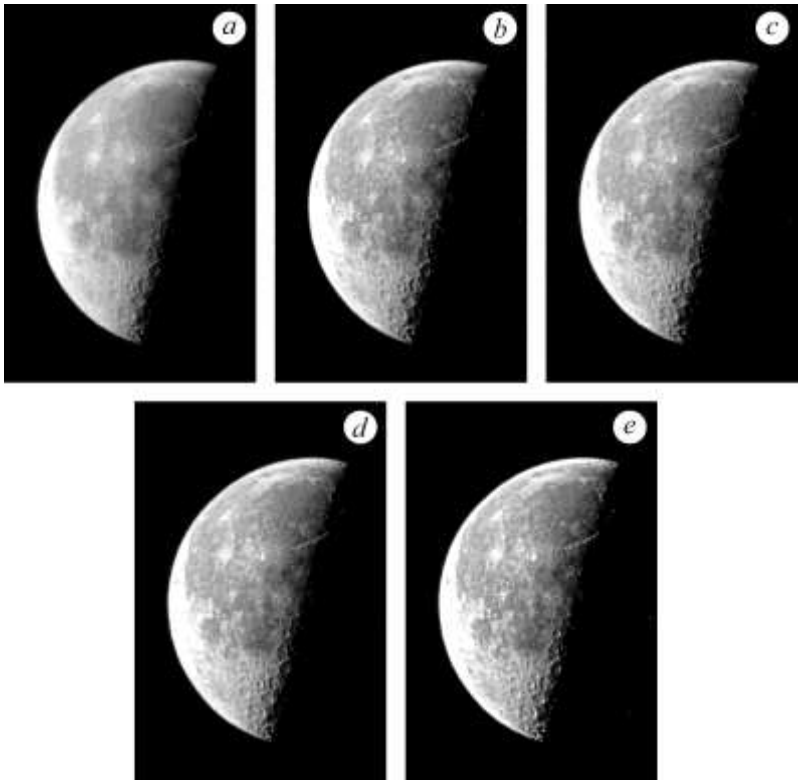

Fig. 4. Input Moon test image (*a*) and results of its enhancement by (16) (*b*), (22) (*c*), (27) (*d*) and proposed method (37) (*e*).

Described above image quality estimation (38) for the input images as well as for the enhanced by known methods (16), (22), (27) and proposed (37) in Figures 1–4 are presented in Tables 1–4.

Table 1. Image characteristics for Cameraman image from Figure 1

Figure	Enhancement type	Q	KC	LQ	KQ	RQ
Fig. 1*a*	Input image	15.858	0.914	0.466	0.507	0.734
Fig. 1*b*	Absolute contrast	22.153	0.949	0.469	0.564	0.883
Fig. 1*c*	Relative contrast	22.477	0.947	0.471	0.572	0.882
Fig. 1*d*	Weighted contrast	22.616	0.946	0.476	0.565	0.889
Fig. 1*e*	Power contrast	25.235	0.969	0.486	0.561	0.955

Table 2. Image characteristics for Pout image from Figure 2

Figure	Enhancement type	Q	KC	LQ	KQ	RQ
Fig. 2*a*	Input image	0.288	0.659	0.433	0.253	0.040
Fig. 2*b*	Absolute contrast	1.413	0.680	0.432	0.386	0.124
Fig. 2*c*	Relative contrast	1.280	0.677	0.432	0.377	0.116
Fig. 2*d*	Weighted contrast	1.712	0.680	0.434	0.383	0.151
Fig. 2*e*	Power contrast	2.678	0.691	0.436	0.412	0.216

Table 3. Image characteristics for Tire image from Figure 3

Figure	Enhancement type	Q	KC	LQ	KQ	RQ
Fig. 3*a*	Input image	8.109	0.880	0.210	0.555	0.789
Fig. 3*b*	Absolute contrast	9.356	0.911	0.212	0.523	0.928
Fig. 3*c*	Relative contrast	9.318	0.907	0.212	0.522	0.927
Fig. 3*d*	Weighted contrast	9.961	0.909	0.220	0.540	0.923
Fig. 3*e*	Power contrast	10.601	0.935	0.232	0.501	0.977

Table 4. Image characteristics for Moon image from Figure 3

Figure	Enhancement type	Q	KC	LQ	KQ	RQ
Fig. 4*a*	Input image	2.768	0.996	0.208	0.388	0.345
Fig. 4*b*	Absolute contrast	3.797	0.996	0.210	0.400	0.454
Fig. 4*c*	Relative contrast	3.530	0.998	0.208	0.391	0.435
Fig. 4*d*	Weighted contrast	3.656	0.997	0.210	0.392	0.446
Fig. 4*e*	Power contrast	4.252	1.000	0.212	0.378	0.530

As it can be seen from above presented Tables 1–4 the image quality estimation measure Q as well as generalized image contrast KC are higher for the images obtained by the proposed method of power enhancement of local image contrasts in comparison with known ones based on absolute, relative and weighted local contrasts.

CONCLUSIONS

A new method of local image contrasts enhancement which is based on the power dependence of the response of the human visual system to light excitation was proposed. The results of the application of the developed method of image quality improvement through the enhancement of local contrasts confirmed its effectiveness compared to the methods based on absolute, relative and weighted local contrasts. This was achieved due to the equalization of the degree of local contrast enhancement caused by the use of a logarithmic scale when presenting the local contrast components. Experimental studies are illustrated by figures and confirmed by image quality estimation measure calculation.

1. Vorobel, R.; Ivasenko, I.; Berehulyak, O. Automatized computer system for evaluation of rust using modified single-scale retinex, In *IEEE First Ukraine Conference on Electrical and Computer Engineering (UKRCON*), Kyiv, Ukraine, 2017, pp 1002–1006. https://doi.org/10.1109/UKRCON.2017.8100401
2. Palenichka, R.M.; Zinterhof, P.; Rytsar, Y.B.; Ivasenko, I.B. Structure-adaptive image filtering using order statistics. *Journal of Electronic Imaging*. **1998**, 7(2). https://doi.org/10.1117/1.482650
3. Lisani, J.L. Adaptive local image enhancement based on logarithmic mappings. In *IEEE International Conference on Image Processing (ICIP)*, 2018. https://doi.org/10.1109/ICIP.2018.8451655
4. Vijayalakshmi, D.; Nath, M.K.; Acharya, O.P. A Comprehensive Survey on Image Contrast Enhancement Techniques in Spatial Domain. *Sensing and Imaging*. **2020**, 21, 40. https://doi.org/10.1007/s11220-020-00305-3
5. Yavorskyy I.M.; Pochapskyy Ye.P.; Vorobel R.A.; Rusyn B.P. Information technologies of nondestructive testing. In *Technical diagnosis of materials and structures*; Nazarchuk Z.T., Ed.; Prostir-M, 2018. (in Ukrainian)
6. Vorobel, R. *Logarithmic Image Processing*; Naukova Dumka, 2012. (in Ukrainian)
7. Pratt, W.K. *Digital Image Processing*; Wiley, 2007. https://doi.org/10.1002/0470097434
8. Mannos, J.L.; Sakrison, D.J. The effects of a visual fidelity criterion on the encoding of images. *IEEE Trans. on Inf. Theory*, **1974**, IT-20(4), 525–536. https://doi.org/10.1109/TIT.1974.1055250
9. Cornsweet, T.N. *Visual Perseption*; Academic Press, 1970.

10. Priest, I.G.; Gibson, K.S.; McNicholas, H.J. An examination of the Munsell color system. 1. Spectral and total reflection on the Munsell scale of value. U.S. National Bureau Standards. Technical paper 167, 1920. https://doi.org/10.6028/nbst.5318
11. Ladd, J.H.; Pinney, J.E. Empirical Relationships with the Muncell value scale. Proc. IRE (Correspondence), 1955, 43(9), 1137. https://doi.org/10.1109/JRPROC.1955.277892
12. Mokrzycki, W.S.; Tatol, M. Colour difference Δ E-A survey. *Mach. Graph. Vis*, **2011**, 20(4), 383–411.
13. Liberini, S.; Rizzi, A. Munsell and Ostwald colour spaces: A comparison in the field of hair colouring. *Color Research & Application*, **2023**, 48(1), 6–20. https://doi.org/10.1002/col.22818
14. Vorobel, R.A. Logarithmic type image processing algebras, In *International Kharkov Symposium on Physics and Engineering of Microwaves, Millimeter and Submillimeter Waves*, Kharkiv, Ukraine, 2010, 1–3. https://doi.org/10.1109/MSMW.2010.5546157
15. Berehulyak, O.; Vorobel, R. The Algebraic Model with an Asymmetric Characteristic of Logarithmic Transformation, In *IEEE 15th International Conference on Computer Sciences and Information Technologies (CSIT)*, Zbarazh, Ukraine, 2020, pp 119–122. https://doi.org/10.1109/CSIT49958.2020.9321906
16. Sheikh, H.R.; Sabir, M.F.; Bovik, A.C. A statistical evaluation of recent full reference image quality assessment algorithms. *IEEE Transactions on Image Processing*. 2006, 15(11), 3441–3452. https://doi.org/10.1109/TIP.2006.881959
17. Egiazarian, K.; Astola, J.; Ponomarenko, N.; Lukin, V.; Battisti F.; Carli, M. New full-reference quality metrics based on HSV. In *Proc. of the Second International Workshop on Video Processing and Quality Metrics*, Scottsdale, USA, 2006, 4 p.
18. Ponomarenko, N. et al. Color image database for evaluation of image quality metrics. *In Proc. IEEE 10thWorkshop on Multimedia Signal Processing*. 2008, 403–408. https://doi.org/10.1109/MMSP.2008.4665112
19. Bringier, B.; Richard, N.; Larabi M.-C.; Fernandez-Maloigne, C. No-reference perceptual quality assessment of color image. In *Proc. 14th European Signal Processing Conference* (*EUSIPCO 2006*), Florence, Italy, September 4–8 2006, 5 p.
20. Zhu T.; Karam, L. A no-reference objective image quality metric based on perceptually weighted local noise, *EURASIP Journal Image Video Process.* **2014**, 1, 1–8. https://doi.org/10.1186/1687-5281-2014-5
21. Choi, L.K.; Bovik, A.C. Video quality assessment accounting for temporal visual masking of local flicker. *Signal Processing: image communication*. **2018**, 67, 182–198. https://doi.org/10.1016/j.image.2018.06.009
22. Ding, K.; Ma, K.; Wang, S.; Simoncelli, E.P. Image quality assessment: Unifying structure and texture similarity. *IEEE transactions on pattern analysis and machine intelligence*. **2020**, 44(5), 2567–2581. https://doi.org/10.1109/TPAMI.2020.3045810
23. Saha, A.; Mishra, S.; Bovik, A.C. Re-IQA: Unsupervised Learning for Image Quality Assessment in the Wild. In *Proceedings of the IEEE/CVF Conference on Computer Vision and Pattern Recognition*, Vancouver, Canada, 2023, pp 5846–5855. https://doi.org/10.1109/CVPR52729.2023.00566
24. Berehulyak, O.; Vorobel, R.; Ivasenko, I. Color Image Enhancement by Logarithmic Transformation in Fuzzy Domain. In *2019 IEEE 2nd Ukraine Conference on Electrical and Computer Engineering (UKRCON)*, Lviv, Ukraine, 2019, pp 1147–1151. https://doi.org/10.1109/UKRCON.2019.8879936

Received 03.09.2024